Case Studies on the Application of the Exhaustive Optimization Method Based on Screening and Zoom Techniques

Alin-Iulian Dolan*

* University of Craiova/Electrical Engineering Faculty, Craiova, Romania, adolan@elth.ucv.ro,
ORCID: 0009-0004-2028-4431

***Abstract* - The present paper presents an exhaustive optimization method based on screening and zoom techniques and its application in two case studies involving electromagnetic devices. The method is based on the design of experiments technique, combining optimization algorithms with numerical simulations. The solution of the optimization problem is performed in two stages: global modeling (coarse optimization) and actual optimization (fine optimization). In the first stage, a partitioning of the entire feasible domain is performed, especially in the areas where there are extrema of the objective function. Their location is signaled by the sign variations of the local effects of the design variables calculated by a screening technique. In the second stage, the actual optimization takes place using the zoom technique, initiated around the point found in the first stage. The paper concludes with two case studies in which the application of the method on 2-D models of electromagnetic devices is exemplified. The optimization problems are to maximize the developed forces while maintaining the overall dimensions and the cross-sections of the coils, depending on two geometric parameters. The method was applied up to zoom level 5, obtaining a considerable improvement in the performances of the electromagnetic devices. The great advantage of the exhaustive method is the determination of the global extremum of the objective function, which becomes all the more expensive the greater the number of design variables and the finer the partitioning.**

Cuvinte cheie: *optimizare globală, tehnică de screening, proiectarea experimentelor, metoda elementului finit bidimensională.*

Keywords: *global optimization, technique of screening, design of experiments, bi-dimensional finite element method.*

I. INTRODUCTION

Modern optimization techniques are directly linked to numerical simulations through the Design of Experiments (DOE) method [1]-[2], in which real experiments are replaced by numerical ones, much cheaper in terms of time and resources. Many recent works prove the success of these tools [3]-[11].

The utility of DOE was demonstrated in [3] for "scanning" a double-cage induction motor to identify the most influential parameters on efficiency and starting torque.

The same technique was applied in [4] to increase the efficiency of a boiler by reducing the gas-steam ratio and in [5] to adjust design variables to optimize a permanent magnet machine.

The multi-objective optimal design of the geometry of a linear switched reluctance motor with segmented motor with segmental mover was obtained in [6] using a combination of DOE and Kriging model.

In [7], a three-parameter multi-objective optimization of graded metal foam under impulsive load was performed, correlating the finite element method (FEM) and DOE.

The paper [8] proposed a robust design for brushless DC motors by using DOE in the driving cycles, overcoming the problems related to manufacturing tolerances.

In [9], DOE was applied to select certain parameters by the Taguchi method in order to optimize a switched reluctance motor for ceiling fan design.

DOE together with genetic algorithms led in [10] to an optimized design of a novel line-start permanent magnet synchronous with double-squirrel-cage structure and fractional slot concentrated winding and the application of FEM was a validation of the obtained solution.

To investigate the effect of bump structures and loading conditions on the electromigration properties of solder bumps in Wafer-level chip-scale packaging, in [11] Ansys, Noesis Optimus, DOE and response surface methodology (RSM) were used. In this way, the effect of passivation opening, thickness of solder surface metallurgy and loading conditions on the electromigration performance of the solder surface was optimized.

Relatively recent concerns in the field of electromagnetic device optimization and screening technique can be found in [12]-[15].

MATLAB software was the tool used in [12] for the geometric optimization of a guide coil to obtain a maximum levitation force, based on very accurate semi-analytical equations, allowing a fast calculation compared to 3D-FEM analysis.

The paper [13] highlights the optimized shape of an electromagnetic actuator of a bionic robot fish, using an adaptive genetic algorithm. Thus, the noise of the electromagnetic drive was reduced and its endurance was extended.

The efficiency of the screening technique is evident from [14] where it was applied to a novel spherical actuator to detect the influence of the main structural parameters on the output torque and on the waveform distortion rate of the system. Their improvement was obtained through a multi-objective optimization using the genetic algorithm.

A preliminary screening study was required in [15] for the optimization of a micro-electro-mechanical system electro-thermal actuator using a multi-objective particle swarm optimization algorithm that takes into account multi-source uncertainties. The effect was to reduce the problem size and obtain a solution with good robustness.

Recent works [16]-[18] illustrate the application of optimization methods based on DOE technique which aim at maximizing the force developed by DC electromagnets.

Complex versions of the methods by zooms and by slidings of designs are applied in [16] to improve the performance of an electromagnetic device with a sufficiently good convergence rate by iteratively using second-order polynomial models.

Among the optimization methods based on DOE, exhaustive methods are distinguished that allow finding the global extremum, in addition to other possible local extrema. They analyze the entire feasible domain, iteratively focusing on the areas that locate the sought extrema. The ways in which these areas are selected make the difference between the methods.

Paper [17] presents, for a similar electromagnetic device, the solution of an optimization problem by the applying of an exhaustive method in which the refinement of the global extremum search uses the analysis of variance (ANOVA) technique.

In [18], another exhaustive optimization method based on screening and zoom techniques is presented, exemplified on the case study in [16].

This paper extends the scope of the method in [18] to the case study in [17].

II. Exhaustive Optimization Method Based on Screening and Zoom Techniques

Exhaustive (global) optimization methods have the great advantage of determining all the extrema of an objective function (local and global), at the cost of a particularly complex calculation.

In cases where its analytical expression and implicitly its derivatives are not available, but only the values of the objective function at the points of the feasible domain, one can resort to optimization methods based on the design of experiments (DOE) technique [2], which are divided into three categories:

- The method based on 1st order factorial designs;
- The method based on 2nd order factorial designs and response surface methodology (RSM);
- The method based on 1st order factorial designs and screening and zoom techniques.

All methods have in common the global modeling of the feasible domain and are also suitable for constrained domains.

The first method uses a predefined distribution of experimental points, independent of the objective function variations. The accuracy of the result depends on the degree of partitioning of the feasible domain.

The second method starts as the first and additionally calculates for each subdomain a second-order polynomial model of the objective function. Depending on the quality of these models, evaluated by RSM adjustment coefficients, it is decided to refine the partitioning in the subdomains with poor quality models and the evaluation process is resumed. The method is the best for identifying the objective function variations, but very expensive for more than 4 parameters.

The last of the methods starts with global modeling and a screening analysis performed at the level of each subdomain. Where changes in the sign of the objective function slopes are observed, the partitioning is refined and the analysis is resumed, until an acceptable optimum point is found.

The algorithm continues with the actual optimization using the zoom technique, which allows for a very precise estimation of the optimum point. The interest of the method increases in the case of a number of parameters greater than 3, when fractional factorial designs become effective.

The third method will be described in detail in the following and will subsequently be exemplified by its application in two case studies involving electromagnetic devices.

A. Global Modeling

In stage I, the global modeling of the feasible domain takes place, which consists of partitioning it into several subdomains in which full factorial designs are created [2]. If N_i is the number of divisions imposed for dimension i ($i = 1 \div k$), the total number of subdomains N_s is:

$$N_s = \prod_{i=1}^{k} N_i \tag{1}$$

These are called basic subdomains and have the associated zoom level $\zeta = 1$.

The partitioning operation defines at the same time a regular discretization network that counts

$$N_p = \prod_{i=1}^{k} (N_i + 1) \tag{2}$$

points. If full factorial designs are performed in each of the N_s subdomains, the total number of experiments quickly becomes very large, especially for large values of k, which leads to an increase in the cost of the experiments. Therefore, it is recommended to use less expensive variants such as fractional factorial designs, Taguchi designs or Placket-Burman designs.

B. Technique of Screening

Technically, screening a system is equivalent to ranking the effects of input factors on its response [1]-[2]. This involves creating a full factorial design, modifying each factor with maximum amplitude. The number of experiments required increases rapidly when the number of factors k becomes large.

The matrix of experiments is a square matrix X of order 2^k. For $k = 2$ we have:

$$X = \begin{pmatrix} +1 & -1 & -1 & +1 \\ +1 & +1 & -1 & -1 \\ +1 & -1 & +1 & -1 \\ +1 & +1 & +1 & +1 \end{pmatrix} \tag{3}$$

If we denote by N_{nk} the number of levels taken by the factor k, we have $N_{n1} = N_{n2} = 2$ (the values +1 and -1 in the

experiment matrix). The number of experiments of the full factorial design will be $N = 2^2 = 4$.

The set of corresponding responses is described by a column vector Y with $2^k = 2^2 = 4$ elements:

$$Y = \begin{pmatrix} Y_1 \\ Y_2 \\ Y_3 \\ Y_4 \end{pmatrix} \tag{4}$$

The effect of factor i on response Y is calculated:

$$E_i = \frac{1}{N} \cdot \sum_{j=1}^{N} \left(X_{j,i+1} \cdot Y_j \right) \tag{5}$$

In stage I of the optimization method, the screening technique is applied for each of the N_s basic subdomains. Adjacent subdomains between which there are sign variations of the effects are searched for and if there are, these will be partitioned into 2^k subdomains and the screening analysis will be resumed for the new subdomains with $\zeta = 2$.

The process can continue until a zoom level imposed by the experimenter is reached, when the optimal experimental point is chosen from the set of obtained points. Stage I represents the coarse optimization stage.

C. Technique of Zoom

In the second stage, the actual optimization takes place through the zoom technique initiated from the point found in the first stage [2].

The simplest version of the zoom methods involves creating a full factorial design around the initial point, delimited by 4 neighboring diagonal points and comparing the values of the objective function in the 5 points, followed by choosing the point with the best value and repeating the action around it.

If the central point offers the best value, the next factorial design will have a zoom level ζ higher by one unit. If not, the same zoom level is maintained.

Stage II represents the fine optimization stage which leads to a very precise estimate of the global maximum of the optimization problem.

III. Application of the Optimization Method on Electromagnetic Devices

In the following, the application of the exhaustive optimization method based on the screening and zoom techniques on DC electromagnetic devices will be exemplified.

A. Case Study I (CS I)

As follows from the design methodology from [19], the initial geometry shape and the values of the main geometric parameters of the device 1 can be followed in Fig. 1 and Table I.

The air gap for which the study was made is $\delta = 41$ mm. The coil has $w = 1269$ turns and the supply voltage is $U_r = 110$ V DC.

The optimization problem has as objective function the actuation force F to be maximized and as design variables the support angle ratio, k_β, and the coil aspect ratio, k_b:

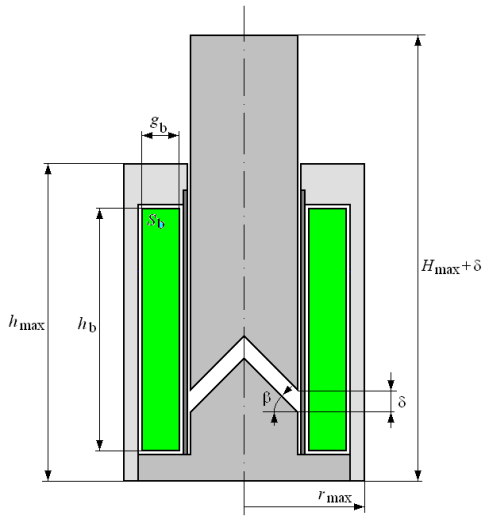

Fig. 1. Initial geometry shape of electromagnetic device 1 (CS I) [16].

TABLE I.
Main Geometrical Parameters of DC Plunger-Type Electromagnet 1 (CS I) [16]

r_1 (mm)	29.80	g_b (mm)	19.83	δ_g (mm)	2.00
r_2 (mm)	0.00	h_b (mm)	138.90	$S_b=g_b \cdot h_b$ (mm^2)	2752.27
r_3 (mm)	29.80	s (mm)	2.00	r_{max}	65.70
β_{in} (°)	45.00	v (mm)	24.29	h_{max}	172.60
a_0 (mm)	9.07	h_b (mm)	192.00	H_{max}	231.19
a_1 (mm)	14.90	b (mm)	10.00		
a_2 (mm)	14.90	δ_p (mm)	1.00		

$$k_\beta = \frac{\beta}{\beta_{in}} \in [0.43 \div 1.56] \tag{6}$$

$$k_b = \frac{h_b}{g_b} \in [6 \div 8] \tag{7}$$

The optimization is subject to four equality constraints that ensure the conservation of the overall dimensions of the device (the external radius r_{max}, the height of carcass h_{max}, the height of plunger + support H_{max}) and the coil cross-section ($S_b = g_b \cdot h_b$). The standard form of the optimization problem (OP_1) is written:

$$OP_1 : \begin{cases} \max F_a(k_\beta, k_b) \\ k_{\beta min} \le k_\beta \le k_{\beta max} \\ k_{bmin} \le k_b \le k_{bmax} \\ g_r(k_b) = 0 \\ g_h(k_b) = 0 \\ g_H(k_b) = 0 \\ g_{Sb}(k_b) = 0 \end{cases} \tag{8}$$

At each iteration n, the gain g_n is calculated compared to the initial value ($n = 0$):

$$g_n = \frac{F_n - F_0}{F_0} \cdot 100\,[\%] \tag{9}$$

The results obtained are presented iteratively in Table II, which also mentions the variation of some

TABLE II.
VARIATION OF PARAMETERS ALONG THE OPTIMIZATION ALGORITHM (CS I) [18]

It.	ζ	N_{tot}	N_{rec}	k_β	k_b	F (N)	g_n (%)	β (°)	g_b (mm)	h_b (mm)
0	-	1	-	1.000	7.000	656.52	-	45.00	19.83	138.80
1	1	64	40	1.566	6.500	775.32	18.09	70.50	20.58	133.75
2	**2**	**128**	**98**	**1.425**	**6.500**	**810.99**	**23.53**	**63.13**	**20.58**	**133.75**
3	2	5	1	1.425	6.500	810.99	23.53	63.13	20.58	133.75
4	3	5	1	1.460	6.438	812.28	23.73	65.72	20.68	133.11
5	3	5	3	1.460	6.438	812.28	23.73	65.72	20.68	133.11
6	4	5	1	1.460	6.438	812.28	23.73	65.72	20.68	133.11
7	**5**	**5**	**1**	**1.452**	**6.422**	**812.47**	**23.75**	**65.32**	**20.70**	**132.95**
Total		218	145							

geometric parameters.

Stage I starts with the initial point P_0 with coordinates $k_\beta = 1$, $k_b = 7$, with the value $F_0 = 656.52$ N and provides the best point P_1 with coordinates $k_\beta = 1.425$, $k_b = 6.5$ and value $F_2 = 810.99$ N, with a gain of 23.53%, at the zoom level $\zeta = 2$.

Figure 2 illustrates the distribution of the basic subdomains ($\zeta = 1$) and Figs. 3 and 4 show the 2-D, respectively 3-D, experimental points and the optimal point for this zoom level. Figure 5 illustrates the distribution of the subdomains with the zoom level $\zeta = 2$ and Figs. 6 and 7 show the experimental points and the optimal point P_1.

Stage II continues with 5 iterations up to point P_2 with coordinates $k_\beta = 1.452$, $k_b = 6.422$ and the value $F_7 = 812.47$ N, with a gain of 23.75%, at zoom level $\zeta = 5$. Figure 8 illustrates the optimization algorithm using the zoom technique, initiated from point P_1. In Figs. 9-10 the entire optimization algorithm is presented, in 2-D and 3-D visualization.

As the optimization results show, none of the design variables reach their range limits. The total number of numerical experiments required was 218, of which 145 were recovered through iterations, leaving 73 experiments actually performed using the FEMM program [20] and the LUA programming language [21]. The force F was determined using the Maxwell Stress Tensor approach.

In Fig. 11 are presented initial and optimal geometry shape and magnetic flux density distribution computed in FEMM software on an axial-symmetric model.

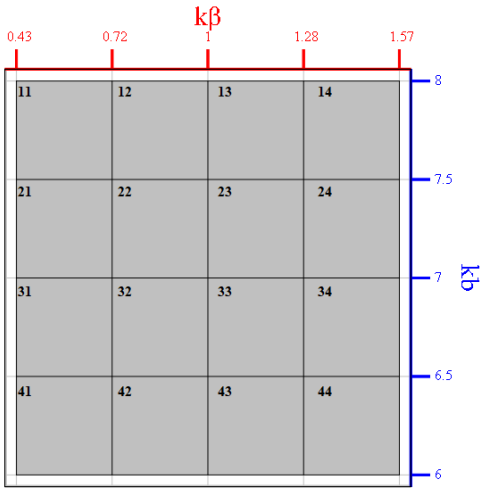

Fig. 2. Distribution of basic subdomains ($\zeta = 1$, CS I) [18].

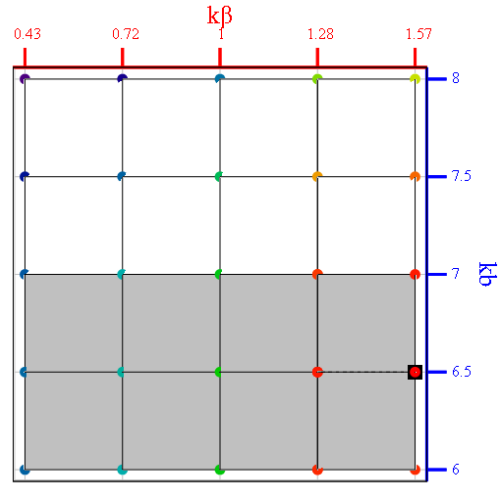

Fig. 3. Experimental points of the basic subdomains ($\zeta = 1$) and the optimal point (in black) for this level (stage I, 2-D view, CS I) [18].

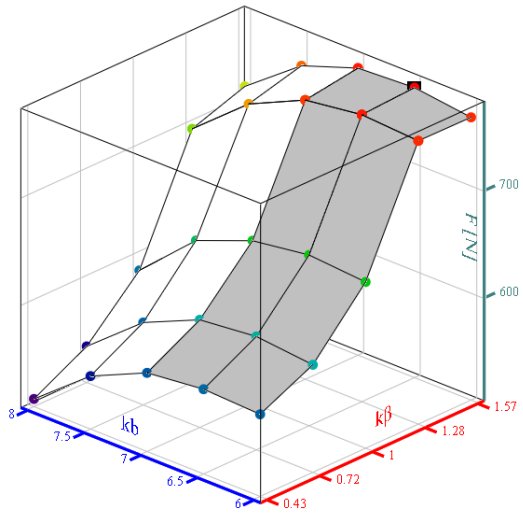

Fig. 4. Experimental points of the basic subdomains ($\zeta = 1$) and the optimal point (in black) for this level (stage I, 3-D view, CS I) [18].

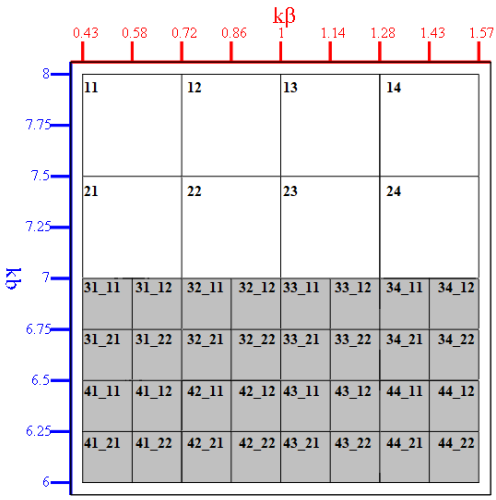

Fig. 5. Distribution of subdomains with zoom level $\zeta = 2$ (CS I) [18].

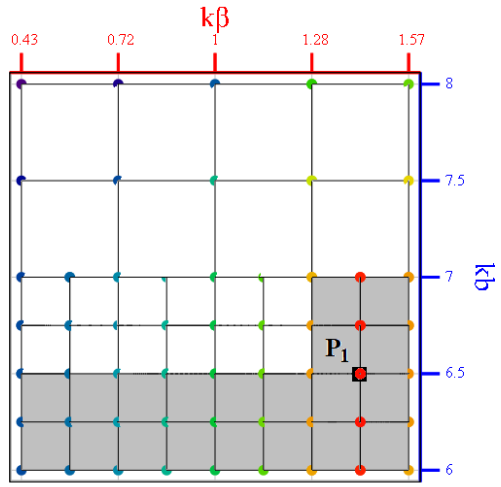

Fig. 6. Experimental points of the subdomains with $\zeta = 2$ and the optimal point P_1 for this level (stage I, 2-D view, CS I) [18].

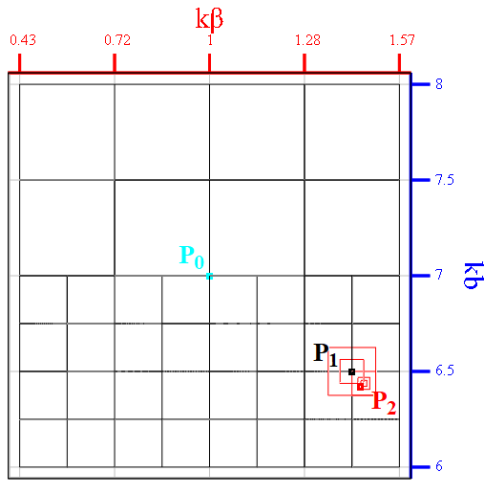

Fig. 9. Optimization algorithm for $\zeta = 1 \div 5$, initial point P_0 and optimal points P_1 (stage I) and P_2 (stage II) (2-D view, CS I) [18].

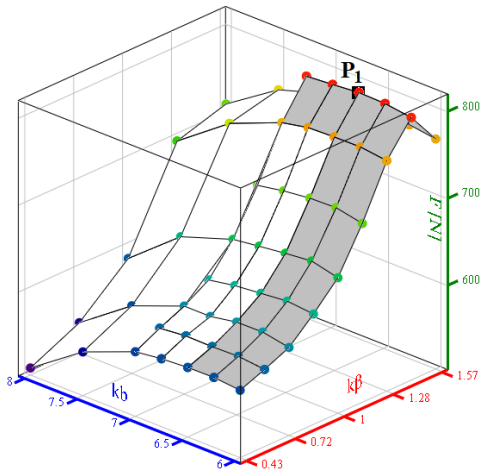

Fig. 7. Experimental points of the subdomains with $\zeta = 2$ and the optimal point P_1 for this level (stage I, 3-D view, CS I) [18].

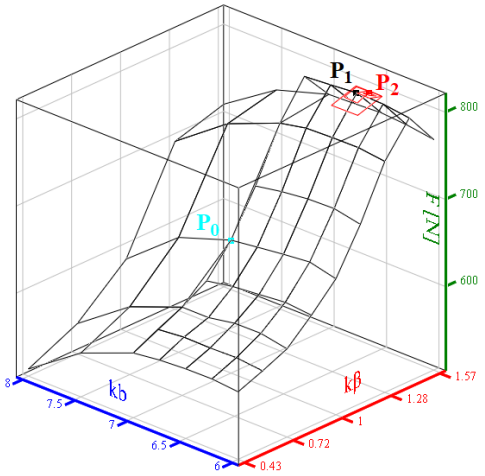

Fig. 10. Optimization algorithm for $\zeta = 1 \div 5$, initial point P_0 and optimal points P_1 (stage I) and P_2 (stage II) (3-D view, CS I) [18].

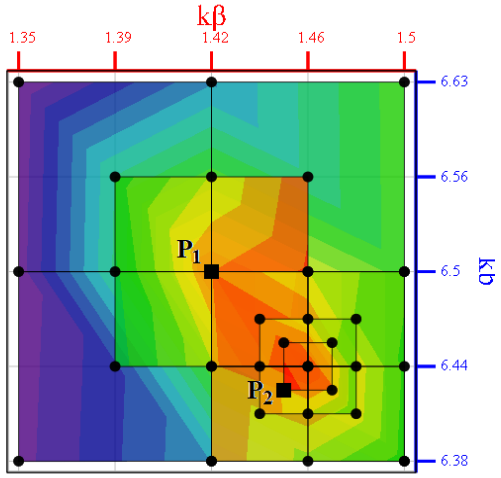

Fig. 8. Experimental points of the subdomains with $\zeta = 2 \div 5$ and the optimal point P_2 for level 5 (stage II, 2-D view, CS I) [18].

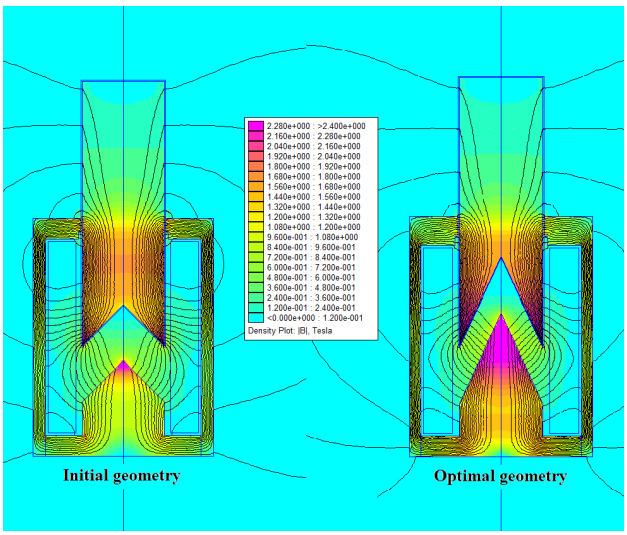

Fig. 11. Initial and optimal geometry shape and magnetic flux density distribution (axial-symmetric solution, FEMM, CS I) [18].

B. Case Study II (CS II)

The initial geometry shape and the values of the main geometric parameters of the device 2 can be followed in Fig. 12 and Table III. The air gap for which the study was made is δ = 1 mm. The coil has w = 11500 turns and the supply voltage is U_r = 115 V DC.

The optimization problem has as objective function the actuation force F to be maximized and as design variables the ratio between the height and thickness of the coil, k_b, and the ratio between the thicknesses of the core yokes, k_{my}:

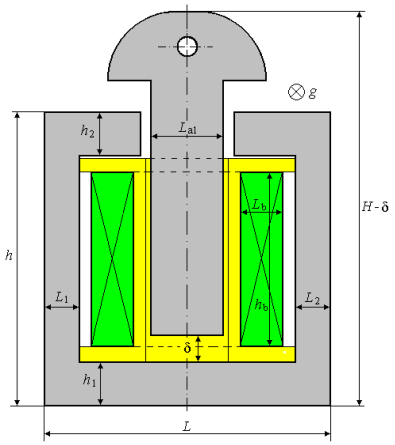

Fig. 12. Initial geometry of electromagnetic device 2 (CS II) [16].

TABLE III.
MAIN GEOMETRICAL PARAMETERS OF DC PLUNGER-TYPE ELECTROMAGNET 2 (CS II) [16]

h (mm)	52.50	**L_{a1in} (mm)**	13.00
H (mm)	65.70	**L_{1in} (mm)**	7.35
L (mm)	50.90	**L_{2in} (mm)**	7.35
S_b=L_b·h_b (mm²)	234.00	**L_{bin} (mm)**	7.50
h_{1in} (mm)	7.90	**h_{bin} (mm)**	31.20
h_{2in} (mm)	7.90	**g (mm)**	19.80

$$k_b = \frac{h_b}{L_b} \in [2 \div 6] \tag{10}$$

$$k_{my} = \frac{h_2}{h_1} \in [0.5 \div 2] \tag{11}$$

The optimization is subject to four equality constraints that ensure the conservation of the overall dimensions of the device (core width L, core height h, total device height H) and the coil cross-section ($S_b = g_b \cdot h_b$). The standard form of the optimization problem (OP_2) is written:

$$OP_2 : \begin{cases} \max F(k_b, k_{my}) \\ k_{b\min} \le k_b \le k_{b\max} \\ k_{my_{\min}} \le k_{my} \le k_{my_{\max}} \\ g_h(k_b, k_{my}) - h = 0 \\ g_L(k_b) - L = 0 \\ g_H(k_b, k_{my}) - H = 0 \\ g_{Sb}(k_b) - S_b = 0 \end{cases} \tag{12}$$

The results obtained are presented iteratively in Table IV, which also mentions the variation of some geometric parameters.

Stage I starts with the initial point P_0 with coordinates k_b = 4, k_{my} = 1.25, with the value F_0 = 22.939 N and provides the best point P_1 with coordinates k_b = 2.5, k_{my} = 2 and value F_2 = 24.924 N, with a gain of 8.66%, at the zoom level ζ = 2.

Figure 13 illustrates the distribution of the basic subdomains (ζ = 1) and Figs. 14 and 15 show the 2-D, respectively 3-D, experimental points and the optimal point for this zoom level. Figure 16 illustrates the distribution of the

TABLE IV.
VARIATION OF PARAMETERS ALONG THE OPTIMIZATION ALGORITHM (CS II)

It.	**ζ**	**N_{tot}**	**N_{rec}**	**k_b**	**k_{my}**	**F (N)**	**g_n (%)**	**L_b (mm)**	**h_b (mm)**	**h_1 (mm)**	**h_2 (mm)**
0	-	1	-	4.00	1.25	22.939	-	7.65	30.59	7.29	9.11
1	1	64	40	3.00	2.00	24.818	8.19	8.83	26.50	6.84	13.67
2	**2**	**128**	**98**	**2.50**	**2.00**	**24.924**	**8.66**	**9.67**	**24.19**	**7.60**	**15.21**
3	2	5	1	2.50	2.00	24.924	8.66	9.67	24.19	7.60	15.21
4	3	5	1	2.63	2.00	24.918	8.63	9.44	24.78	7.41	14.81
5	3	5	3	2.50	2.00	24.924	8.66	9.67	24.19	7.60	15.21
6	4	5	3	2.63	2.00	24.918	8.63	9.44	24.78	7.41	14.81
7	**5**	**5**	**3**	**2.50**	**2.00**	**24.924**	8.66	**9.67**	**24.19**	**7.60**	**15.21**
Total		218	149								

subdomains with the zoom level ζ = 2 and Figs. 17 and 18 show the experimental points and the optimal point P_1.

Stage II continues with 5 iterations up to point P_2 with coordinates k_b = 2.5, k_{my} = 2 and value F_7 = 24.924 N, with a gain of 8.66%, at zoom level ζ = 5. Figure 19 illustrates the optimization algorithm using the zoom technique, initiated from point P_1. In Figs. 20-21 the entire optimization algorithm is presented, in 2-D and 3-D visualization.

As the optimization results show, one of the design variables reaches its range limit. The total number of numerical experiments required was 218, of which 149 were recovered through iterations, leaving 69 experiments actually performed using the FEMM program [20] and the LUA programming language [21]. The force F was determined using the Maxwell Stress Tensor approach.

In Fig. 22 are presented initial and optimal geometry shape and magnetic flux density distribution computed in FEMM software on a planar model.

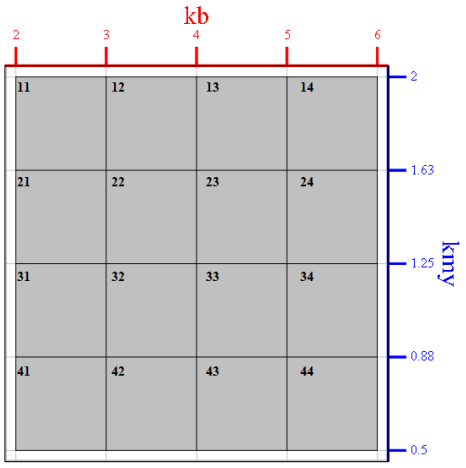

Fig. 13. Layout of basic subdomains (ζ = 1, CS II).

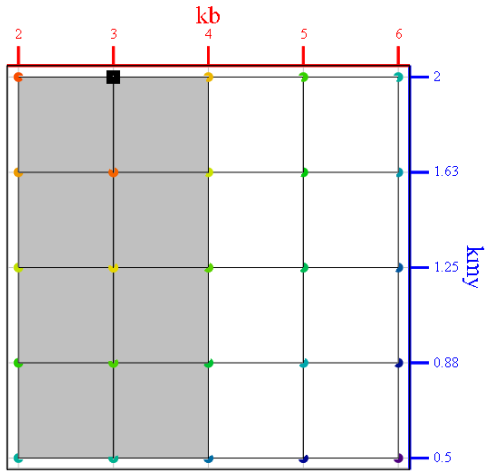

Fig. 14. Experimental of the basic subdomains ($\zeta = 1$) and the optimal point (in black) for this level (stage I, 2-D view, CS II).

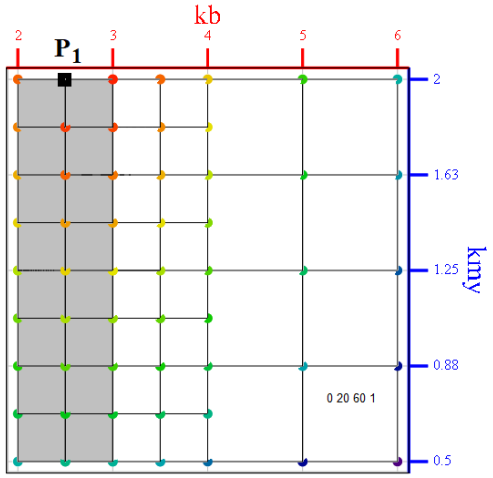

Fig. 17. Experimental points of the subdomains with $\zeta = 2$ and the optimal point P_1 for this level (stage I, 2-D view, CS II).

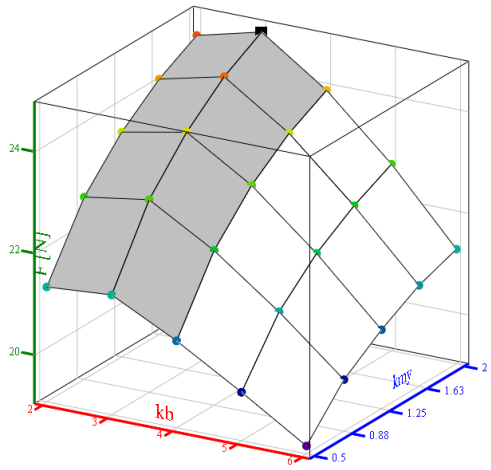

Fig. 15. Experimental points of the basic subdomains ($\zeta = 1$) and the optimal point (in black) for this level (stage I, 3-D view, CS II).

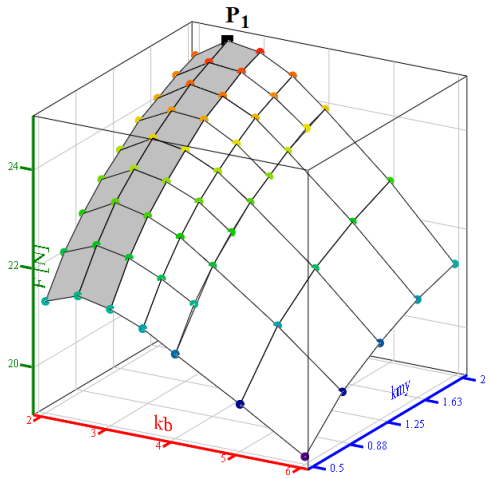

Fig. 18. Experimental points of the subdomains with $\zeta = 2$ and the optimal point P_1 for this level (stage I, 3-D view, CS II).

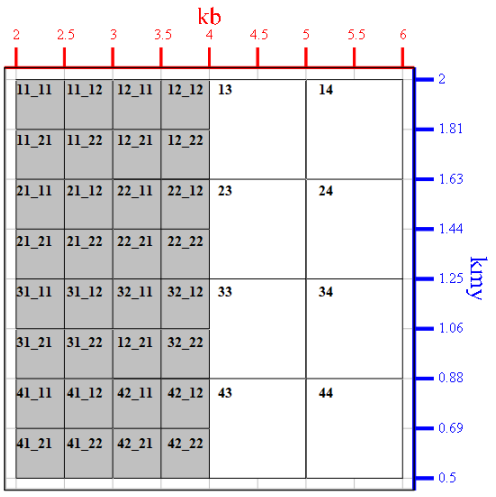

Fig. 16. Distribution of subdomains with zoom level $\zeta = 2$ (CS II).

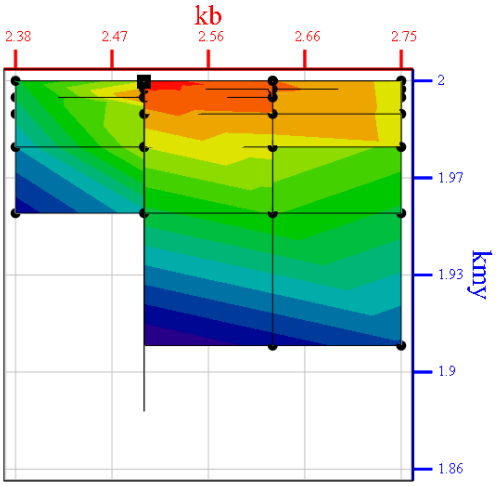

Fig. 19. Experimental points of the subdomains with $\zeta = 2 \div 5$ and the optimal point P_2 for level 5 (stage II, 2-D view, CS II).

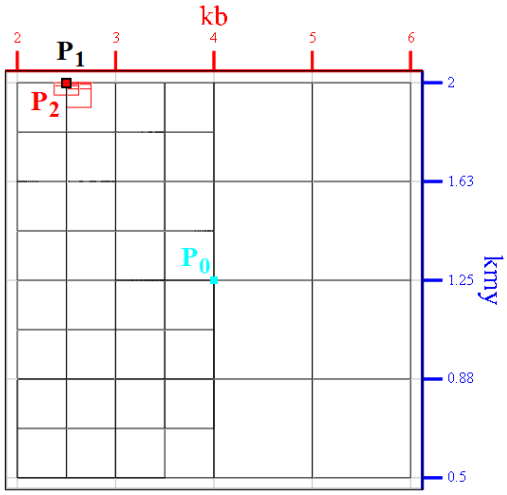

Fig. 20. Optimization algorithm for $\zeta = 1 \div 5$, initial point P_0 and optimal points P_1 (stage I) and P_2 (stage II) (2-D view, CS II).

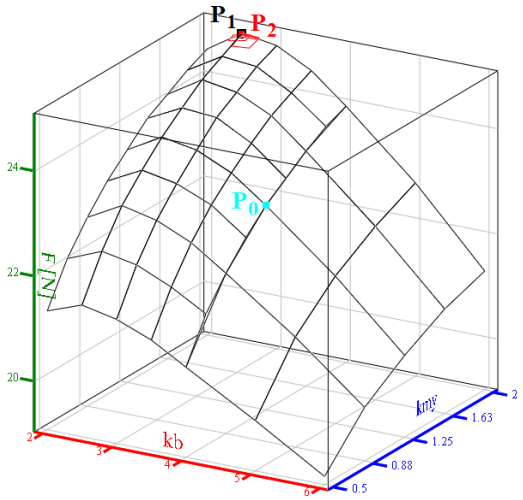

Fig. 21. Optimization algorithm for $\zeta = 1 \div 5$, initial point P_0 and optimal points P_1 (stage I) and P_2 (stage II) (3-D view, CS II).

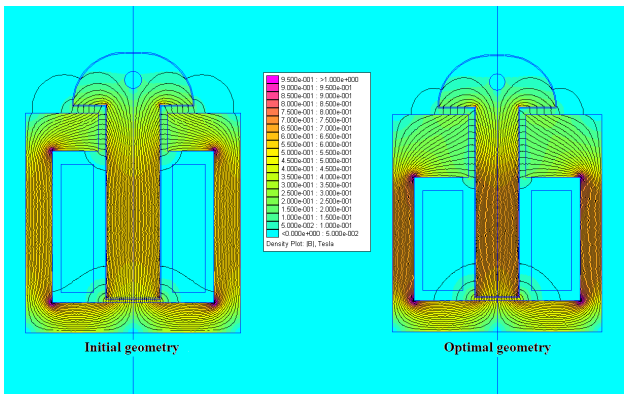

Fig. 22. Initial and optimal geometry shape with magnetic flux density distribution (planar solution, FEMM, CS II).

IV. Conclusions

In this paper, an exhaustive optimization method based on screening and zoom techniques from the field of experimental design was presented. The method is structured in two stages. The first represents a global modeling of the feasible domain, with a higher degree of refinement in the subdomains where changes in the slope of the objective function are found, through screening analyses. The second stage is the actual optimization using the zoom technique to improve the result of the first stage.

The application of the method was exemplified in two case studies of electromagnetic devices for which 2-D numerical models were obtained using the FEMM program. In the first case study, in the global modeling stage, 23.53% was gained and in the actual optimization stage, the percentage increased to 23.75% of the initial value. In the second case study, the gain was obtained only in the global modeling stage, of 8.66%, but it did not improve in the second stage.

Thanks to the second stage of actual optimization through the zoom technique, the presented method proves to be very accurate compared to other exhaustive methods.

From the point of view of the magnetic circuit, the solution obtained for the first case leads to a pronounced saturation of the plunger and its support, which indicates the need to take into account the saturation level as an additional design variable. The geometric asymmetry of the solution for the second case may have some consequences from the point of view of mechanical stability, which would require reducing the upper limit of the design variable k_{my}.

Acknowledgment

Source of research funding in this article: Research program of the Electrical Engineering Department financed by the University of Craiova.

Contribution of authors:
First author – 100%

Received on September 25, 2025
Editorial Approval on December 2, 2025

References

[1] D. Montgomery, *Design and Analysis of Experiment*, 5-th Edition, Arizona State University, 2000.

[2] S. Vivier, *Optimization Strategies Using the Design of Experiments Method and Applications to Electrotechnical Devices Modeled by Finite Elements* (In French), Ph-D Thesis, Lille, 2002.

[3] A.-I. Constantin, and V. Fireteanu, "HyperSudy optimization of induction motors finite element assisted design," International Aegean Conference on Electrical Machines and Power Electronics (ACEMP) & 2021 International Conference on Optimization of Electrical and Electronic Equipment (OPTIM), pp. 191-197, 2021, doi: 10.1109/OPTIM-ACEMP50812.2021.9590030.

[4] L. Liu, K. Xu, X. He, and X. Cao, "Energy-saving optimization of the gas-fired boiler by DOE method," Proceedings of the X-th International Forum on Electrical Engineering and Automation (IFEEA), Nanjing, China, pp. 8-12, 2023, doi: 10.1109/IFEEA60725.2023.10429450.

[5] N. Taran, V. Rallabandi, D.-M. Ionel, G. Heins, D. Patterson, and P. Zhou, "Design optimization of electric machines with 3-D FEA and a new hybrid DOE-DE numerical algorithm," Proceedings of IEEE International Electric Machines & Drives Conference

(IEMDC), May 12-15, San Diego, CA, USA, pp. 603-608, 2019, doi: 10.1109/IEMDC.2019.8785088.

[6] X. Yi, C. Zhu, C. Huang, D. Wang, and X. Wang, "Design optimization of linear switched reluctance motor with segmental mover," XIII-th Int. Symposium on Linear Drives for Industry Applications (LDIA), July 01-03, Wuhan, China, pp. 1-6, 2021, doi: 10.1109/LDIA49489.2021.9505921.

[7] A. Bassiri Nia, M.Y. Yahya, and A. Faraokhi Nejad, "Optimization of graded metallic foam subjected to impulsive loading through DOE approach," IX-th International Conference on Mechanical and Aerospace Engineering, July 10-13, Budapest, Hungary, pp. 295-299, 2018, doi: 10.1109/ICMAE.2018.8467559.

[8] F. Mahmouditabar, A. Vahedi, and N. Takorabet, "Robust design of BLDC motor considering driving cicle," *IEEE Transaction on Transp. Electrification*, Vol. 10, No. 1, pp. 1414-1424, March, 2024, doi: 10.1109/TTE.2023.3285650.

[9] V.K. Singh, and B. Singh, "Design and development of efficient energy outer rotor switched reluctance motor for ceiling fan," IEEE International Electric Machines & Drive Conference (IEDMC), May 15-18, San Francisco, USA, pp. 1-7, 2023, doi: 10.1109/IEMDC55163.2023.10238847.

[10] X. Li, J. Gong, X. Wang, N. Bracikowski, and F. Gillon, "Proposal of a novel line-start permanent magnet synchronous machine using fractional slot concentrated winding," XXVI-th International Conference on Electrical Machines and Systems (ICEMS), Nov. 05-08, Zhuhai, China, pp. 3027-3032, 2023, doi: 10.1109/ICEMS59686.2023.10344658.

[11] L. Du, S. Deng, Z. Cui, R. Poelma, C. Beelen-Hendrikx, and K. Zhang, "Multi-parameters optimization for electromigration in WLCSP solder bumps," XXV-th International Conference on Thermal, Mechanical and Multi-Physics Simulation and Experiments in Microelectronics and Microsystems (EuroSimE), April 07-10, Catania, Italy, pp. 1-4, 2024, doi: 10.1109/EuroSimE60745.2024.10491411.

[12] M. Lahdo, T. Ströhla, and S. Kovalev, "Magnetically levitated planar positioning systems based on Lorentz forces," 11th International Symposium on Linear Drives for Industry Applications (LDIA), September, 06-08, Osaka, Japan, pp. 1-6, 2017, doi: 10.23919/LDIA.2017.8097232.

[13] H. Zhu, Z. Zhang, R. Zhang, Y. Gao, M. Yang, Y. Li, X. Ni, T. Zhou, S. Zhang, and C. Zhu, "Optimization design of electromagnetic actuator for bionic robotic fish based on genetic algorithm," International Conference on Machine Learning, Control, and Robotics (MLCR), October, 29-31, Suzhou, China, pp. 148-152, 2022, doi: 10.1109/MLCR57210.2022.00035.

[14] L. Zhang, L.Yan, and Z. Dong, „Optimization of a novel spherical actuator with 3-D DOF motion," 18th Conference on Industrial Electronics and Applications (ICIEA), September, 11, Ningbo, China, pp. 1-6, 2023, doi: 10.1109/ICIEA58696.2023.10241512.

[15] H. Zhu, Y. Cao, X. Kong, S. Lei, H. Lu, W. Nie, and Z. Xi, „Selecting robust multi-objective optimization of a MEMS electrothermal actuator considering multi-source uncertainties," *IEEE Transaction on Electron Devices*, Vol. 70, No. 7, pp. 3820-3827, 2023, doi: 10.1109/TED.2023.3278621.

[16] A.-I. Dolan, "Polynomial models used in optimization by design of numerical experiments", *Annals of the University of Craiova, Series: Electrical Engineering*, No. 48, Issue 1, Universitaria Publishing House, pp. 46-54, 2024, doi: 10.52846/AUCEE.2024.07.

[17] A.-I. Dolan, "Exhaustive optimization method applied on electromagnetic device," *Annals of the University of Craiova, Series: Electrical Engineering*, No. 46, Issue 1, Universitaria Publishing House, pp. 34-41, 2022, doi: 10.52846/AUCEE.2022.06.

[18] A.-I. Dolan, "Exhaustive optimization method based on screening and zoom techniques applied to an electromagnetic device", Proceedings of the XV-th International Conference on Electromechanical and Power Systems (SIELMEN 2025), October 15-17, Iasi-Chisinau, pp. 531-536, 2025, doi: 10.1109/SIELMEN67352.2025.11260691.

[19] G. Hortopan, *Electrical Apparatus of Low Voltage* (in Romanian), Bucharest: Tehnica Publishing House, 1969.

[20] https://www.femm.info/wiki/HomePage

[21] https://www.lua.org/